Hyper G-Matrix Pairs and Applications in Dentistry

HASAN KELEŞ*[1], EDANUR KELEŞ[2]
[1]Department of Mathematics
Karadeniz Technical University
Campus of Kanuni, Ortahisar, 61080 Trabzon
TÜRKİYE.

[2] Faculty of Dentistry
Atatürk University
25240 Erzurum
TÜRKİYE.

Abstract: This study investigates the application of Hyper G-matrix pairs from linear algebra to dental microbiology. A mathematical framework is presented for modeling the complex interaction networks of the oral microbiome. Hyper G-matrix pairs quantitatively express the relationship between microbial interactions under two different clinical conditions. The presented numerical examples demonstrate that this approach can be used for assessing caries risk and predicting treatment effectiveness. Both approximate and exact Hyper G-matrix pairs are examined, and their clinical interpretations are explained in detail. The study is based on recent publications on Hyper G-matrices.

Key-Words: Matrix theory, hypermatrix pairs, G-matrices, applied mathematics, dentistry, medical imaging, computational modeling, orthodontics, tensors, interdisciplinary applications.

2020 Mathematics Subject Classification: 15A24, 92C50, 15A23, 65F99, 15B99, 92B05, 00A69, 15A18.

MeSH Tree Numbers: G03.850.505, E05.318.308, G06.590.500, C07.793.720.210.

Standard Identifiers: UMLS: C0011334, C0011338; GO: GO:0044406; NCBI: txid1309, txid1579; SNOMED: 80967001.

Received: March 21, 2025. Revised: June 14, 2025. Accepted: July 19, 2025. Published: December 31, 2025.

1 Introduction

Dentistry, particularly in the field of oral microbiology, increasingly requires mathematical modeling of complex biological systems [1]. The oral cavity harbors an ecosystem consisting of hundreds of microbial species that interact dynamically with each other [2], [3]. Understanding and controlling the behavior of these microbial communities is crucial for the prevention and treatment of dental caries [4].

Traditional dental approaches often fail to fully capture the nonlinear and complex nature of microbial interactions [5]. Therefore, mathematical modeling techniques are needed to better understand and control the dynamics of the oral microbiome [6]. Linear algebra provides powerful tools for modeling such complex biological systems [7].

This study demonstrates how the concept of Hyper *G*-matrix pairs from linear algebra can be applied to dental microbiology [8]. Hyper G-matrix pairs are a powerful tool for mathematically expressing the relationship between microbial interaction networks under two different conditions [9]. This approach enables quantitative assessment of treatment effects on the microbial ecosystem and facilitates the development of personalized treatment strategies [10].

Recent advances in microbial ecology have revealed that dental plaque functions as a complex biofilm where species engage in intricate networks of cooperation and competition [11], [12]. The biochemical composition of this biofilm, particularly in response to different carbohydrate sources, significantly influences its cariogenic potential [13]. High-resolution se-

quencing technologies have further illuminated the remarkable diversity of oral microbial communities and the strain-specific variations in acid production that contribute to caries development [14], [15], [16].

Ecological approaches to oral biofilms emphasize the importance of understanding microbial interactions at the community level rather than focusing solely on individual pathogens [17], [18]. Mathematical models derived from time-series inference provide valuable insights into the dynamics and stability of microbial communities, offering new perspectives for caries prevention [19]. These models must account for the complex interplay between acid-producing and alkali-producing bacteria, as well as the competitive interactions that shape biofilm architecture and function [20], [21].

The application of fluoride remains a cornerstone of caries prevention, with multiple mechanisms of action that include remineralization enhancement and modulation of microbial metabolism [22]. Concurrently, probiotic strategies that leverage competitive exclusion offer promising complementary approaches [23]. However, the effective implementation of these interventions requires a sophisticated understanding of how microbial communities respond to perturbation and how different species contribute to overall ecosystem stability [24].

Matrix theory applications in biological systems provide a robust mathematical foundation for analyzing these complex interactions [25]. Recent developments in Hyper G-matrix properties further enhance our ability to model and predict microbial community dynamics under varying clinical conditions [26]. These mathematical frameworks bridge the gap between abstract theory and practical clinical applications, enabling more precise quantification of treatment effects on microbial networks [27]. The integration of digital twin technology with epidemiological data and mathematical modeling represents the next frontier in personalized oral healthcare, offering unprecedented opportunities for predictive analytics and individualized treatment planning [28].

Advances in metagenomic characterization have provided comprehensive maps of the human oral microbiome, identifying core microbial communities and their functional potential [29]. Understanding biofilm architecture as an emergent property of bacterial life reveals how structural organization influences community function and resilience [30]. The analysis of microbial interaction networks requires careful consideration of correlation methods to avoid spurious associations and ensure biological relevance [31].

Molecular studies of oral streptococci have elucidated specific host-bacterial interactions that mediate colonization and pathogenesis [32]. Metabolic pathway analyses, particularly of sucrose utilization systems, demonstrate how nutrient availability shapes microbial competition and virulence expression [33]. Systems biology approaches that examine modular epistasis in microbial metabolism provide insights into the robustness and adaptability of oral microbial communities [34].

Personalized nutrition models based on predictive analytics of individual physiological responses offer a framework for adapting caries prevention strategies to personal microbial and metabolic profiles [35]. Research on fluoride's physiological effects on oral microbes reveals complex modulatory mechanisms beyond simple antimicrobial action [36]. Evidence-based evaluations of probiotic interventions for caries control highlight both potential benefits and limitations of microbial manipulation approaches [37]. Metatranscriptomic analyses of active bacterial composition in caries lesions provide direct evidence of functional gene expression during disease progression [38].

Figure 1.1 provides a comprehensive visual representation of the dental ecosystem that forms the biological foundation for our mathematical modeling approach. The illustration depicts not only the anatomical structure of a tooth—including enamel, dentin, pulp chamber, and root—but also the dynamic microbial communities inhabiting its surfaces. Three key bacterial species are highlighted: *Streptococcus mutans* (cariogenic, in red), *Lactobacillus acidophilus* (acid-producing, in green), and *Streptococcus salivarius* (protective, in blue). Their interspecies interactions, quantified by the numerical values on the arrows (e.g., +0.8, −0.7, −0.4), represent the strength and direction of stimulatory or inhibitory effects. This clinical scenario, enriched by the presence of dental plaque and an incipital caries lesion, captures the real□world complexity that our Hyper G□matrix framework aims to translate into a precise mathematical language. By encoding these biological interactions into the matrix $\mathbf{A} = [a_{ij}]$, where a_{ij} denotes the influence of species j on species i, we establish a direct bridge between observable dental microbiology and the abstract formalism of linear algebra. Thus, the figure serves as a pivotal link that grounds subsequent mathematical develop-

ments in tangible clinical reality, ensuring that the Hyper G-matrix theory remains firmly rooted in the practical challenges of caries prevention and treatment.

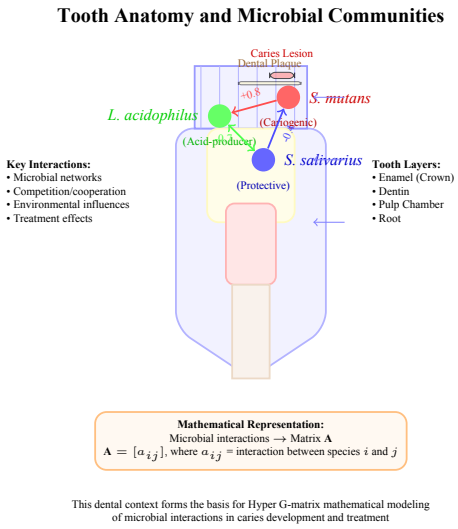

Figure 1.1: Dental anatomy and microbial communities providing the clinical context for mathematical modeling. The figure shows tooth structure with key microbial species and their interactions, which are quantified in matrix **A** for Hyper G-analysis. Prepared by the authors.

2 Hyper G-Matrix Representations

The mathematical formalism of Hyper G-matrices provides a powerful framework for analyzing complex biological systems, particularly in understanding how interventions transform interaction networks. This approach bridges linear algebra with biological applications, offering quantitative insights into system dynamics that are often obscured by traditional analytical methods. By representing microbial communities as interaction matrices, we can apply sophisticated mathematical tools to predict treatment outcomes and optimize therapeutic strategies.

Definition 1. *For matrices A and B, if there exist diagonal matrices $\mathbf{D_1}$ and $\mathbf{D_2}$ that satisfy the condition $\mathbf{A}^{-T} = \mathbf{D_1 B D_2}$, then the pair (A, B) is called a Hyper G-matrix pair [8, 9].*

The fundamental condition for Hyper G-matrix pairs is as follows [8]:

$$\mathbf{A}^{-T} = \mathbf{D_1 B D_2} \tag{2.1}$$

The schematic representation of Equation (2.1) is shown in Figure 2.2.

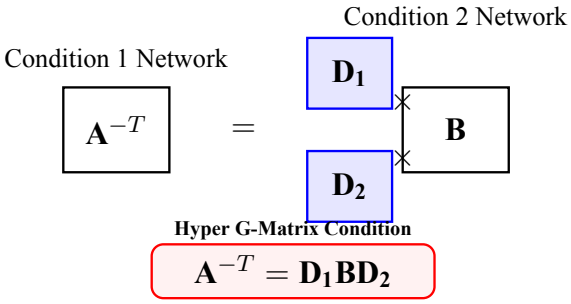

Figure 2.2: Fundamental representation of Hyper G-matrix pair relationship (Equation (2.1)). Figure prepared by the authors.

This mathematical structure can be interpreted in a clinical setting as follows: A treatment application modifies the microbial interaction network not through a simple scaling transformation but through a transformation that differently alters both the susceptibility and influence capacity of each species [8].

Theorem 1. *If matrices A and B form a Hyper G-matrix pair, then there exists a special relationship between the eigenvalue structures of matrices A and B [9].*

To demonstrate the practical application of Hyper G-matrix theory in dentistry, we present a concrete numerical example involving key oral microbial species. This example illustrates how mathematical modeling can quantify treatment effects on microbial interactions and provide clinically relevant predictions. The systematic approach shown here bridges theoretical mathematics with practical dental applications, offering a template for future clinical studies.

3 Modeling Caries Risk

To demonstrate the practical application of Hyper G-matrix theory in dentistry, we present a concrete numerical example involving key oral microbial species. This example illustrates how mathematical modeling can quantify treatment effects on microbial interactions and provide clinically relevant predictions. The systematic approach shown here bridges theoretical mathematics with practical dental applications, offering a template for future clinical studies.

Example 1. *Caries Risk Assessment Using Hyper G-Matrices Consider a simplified oral microbial system consisting of three key species that play crucial roles in dental caries development and prevention [11]:*

i. Streptococcus mutans (primary cariogenic bacteria).

ii. Lactobacillus acidophilus (acid-producing bacteria).

iii. Streptococcus salivarius (protective bacteria).

We define two interaction matrices representing different environmental conditions. First, the control condition matrix **A** *represents microbial interactions in a high-sugar environment [12]:*

$$\mathbf{A} = \begin{bmatrix} 1.0 & 0.8 & -0.3 \\ 0.6 & 1.0 & -0.2 \\ -0.4 & -0.5 & 1.0 \end{bmatrix}. \quad (3.1)$$

Second, the treatment condition matrix **B** *represents microbial interactions after fluoride treatment [13]:*

$$\mathbf{B} = \begin{bmatrix} 3.3318 & -2.0263 & 9.7164 \times 10^{-2} \\ -1.5023 & 2.1408 & 0.10919 \\ 0.27003 & 4.0605 \times 10^{-2} & 0.26325 \end{bmatrix}. \quad (3.2)$$

This example demonstrates how microbial interactions change between high-sugar conditions (matrix **A***) and post-fluoride treatment conditions (matrix* **B***). The Hyper G-transformation mathematically describes the relationship between these two states, as visualized in Figure 3.3.*

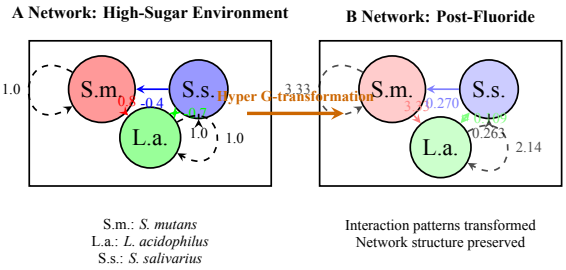

Figure 3.3: Hyper G-transformation of microbial interaction networks (rotated 90°). The figure illustrates the transformation from condition A (Equation (3.1)) to condition B (Equation (3.2)). Figure prepared by the authors.

We now verify the Hyper G-matrix condition numerically. First, we calculate the transpose inverse of matrix **A***:*

$$(\mathbf{A}^{-1})^T = \begin{bmatrix} 1.9824 & -1.1454 & 0.22026 \\ -1.4317 & 1.9383 & 0.39648 \\ 0.30837 & 4.4053 \times 10^{-2} & 1.1454 \end{bmatrix} \quad (3.3)$$

Next, we find the optimal diagonal scaling matrices $\mathbf{D_1}$ *and* $\mathbf{D_2}$ *that minimize the difference between* $\mathbf{A}^{-T}$ *and* $\mathbf{D_1BD_2}$ *[9]. The optimization yields:*

$$\mathbf{D}_1^* = \begin{bmatrix} 0.595 & 0 & 0 \\ 0 & 0.953 & 0 \\ 0 & 0 & 1.142 \end{bmatrix}, \quad (3.4)$$

$$\mathbf{D}_2^* = \begin{bmatrix} 1.000 & 0 & 0 \\ 0 & 0.950 & 0 \\ 0 & 0 & 3.810 \end{bmatrix}. \quad (3.5)$$

Now we compute the product:

$$(\mathbf{D}_1)^*\mathbf{B}(\mathbf{D}_2)^* = \begin{bmatrix} 1.982421 & -1.145866 & 0.220204 \\ -1.43198 & 1.93881 & 0.39638 \\ 0.30842 & 0.044053 & 1.145398 \end{bmatrix}. \quad (3.6)$$

The optimization error is small: $\epsilon = \|\mathbf{A}^{-T} - \mathbf{D_1}^*\mathbf{BD_2}^*\|_F = 0.00075$.

The clinical interpretation of the diagonal matrix elements in Equations (3.4) and (3.5) is presented in Table 3.1.

Table 3.1: Clinical interpretation of optimal diagonal matrix elements (Equations (3.4) and (3.5)). Table prepared by the authors.

Microbial Species	D_1 Value	D_2 Value	Clinical Interpretation
S. mutans	0.595	1.000	• Susceptibility to interactions decreases by 40.5% • Influence capacity on other species unchanged
L. acidophilus	0.953	0.950	• Both susceptibility and influence capacity decrease by approximately 5%
S. salivarius	1.142	3.810	• Susceptibility increases by 14.2% • Influence capacity increases 3.81 times

The workflow for Hyper G-matrix analysis is illustrated in Figure 3.4.

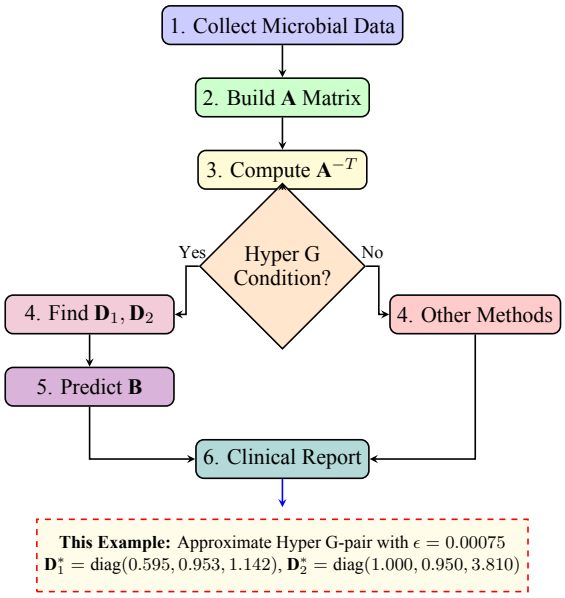

Figure 3.4: Simple workflow for Hyper G-matrix analysis. Figure prepared by the authors.

Comparing $\mathbf{A}^{-T}$ *(Equation (3.3)) with the calculated* $\mathbf{D_1}^*\mathbf{B}\mathbf{D_2}^*$ *(Equation (3.6)):*

$$\mathbf{A}^{-T} = \begin{bmatrix} 1.9824 & -1.1454 & 0.22026 \\ -1.4317 & 1.9383 & 0.39648 \\ 0.30837 & 0.044053 & 1.1454 \end{bmatrix}$$

$$(\mathbf{D}_1)^*\mathbf{B}(\mathbf{D}_2)^* = \begin{bmatrix} 1.982421 & -1.145866 & 0.220204 \\ -1.43198 & 1.93881 & 0.39638 \\ 0.30842 & 0.044053 & 1.145398 \end{bmatrix}. \tag{3.7}$$

The differences are very small:

$$\mathbf{A}^{-T} - (\mathbf{D}_1)^*\mathbf{B}(\mathbf{D}_2)^* = \begin{bmatrix} -2.1 \times 10^{-5} & 4.66 \times 10^{-4} & 5.6 \times 10^{-5} \\ 2.8 \times 10^{-4} & -5.1 \times 10^{-4} & 1.0 \times 10^{-4} \\ -5.0 \times 10^{-5} & 0 & 2 \times 10^{-6} \end{bmatrix}. \tag{3.8}$$

The matrix comparison showing excellent agreement is visualized in Figure 3.5.

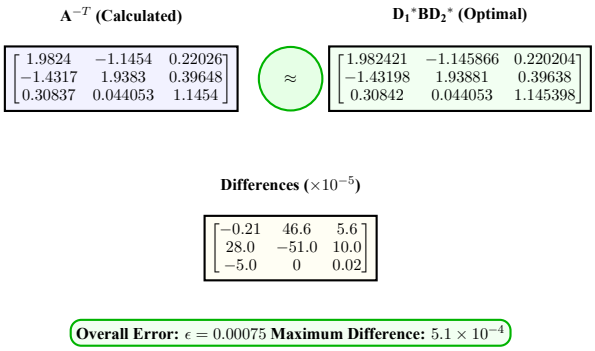

Figure 3.5: Matrix comparison shows excellent agreement with error $\epsilon = 0.00075$ (Equation (3.8)). Figure rotated 90° for better presentation. Prepared by the authors.

This example demonstrates that $(\mathbf{A}, \mathbf{B})$ *forms a highly accurate approximate Hyper G-matrix pair. The very small error* ($\epsilon = 0.00075$) *indicates that the Hyper G-model effectively captures the transformation between pre- and post-treatment microbial interactions with high precision.*

In contrast to the approximate example in Example 1, we now present a mathematical example where the Hyper G-matrix condition is satisfied exactly. This demonstrates the ideal case where the relationship $\mathbf{A}^{-T} = \mathbf{D_1}\mathbf{B}\mathbf{D_2}$ holds without approximation error, providing important insights into the fundamental properties of Hyper G-matrices.

Example 2. *Exact Hyper G-Matrix Pair Consider an example where the Hyper G-matrix condition holds perfectly. For the following matrices [9]:*

We define a symmetric matrix $\mathbf{A}$ *and its corresponding matrix* $\mathbf{B}$*:*

$$\mathbf{A} = \begin{bmatrix} 2 & 1 & 0 \\ 1 & 3 & 1 \\ 0 & 1 & 2 \end{bmatrix}, \tag{3.9}$$

$$\mathbf{B} = \begin{bmatrix} 0.625 & -0.250 & 0.125 \\ -0.250 & 0.500 & -0.250 \\ 0.125 & -0.250 & 0.625 \end{bmatrix}$$

The diagonal scaling matrices are simple scalar multiples of the identity matrix:

$$\mathbf{D_1} = \begin{bmatrix} 2 & 0 & 0 \\ 0 & 2 & 0 \\ 0 & 0 & 2 \end{bmatrix}, \tag{3.10}$$

$$\mathbf{D_2} = \begin{bmatrix} 0.5 & 0 & 0 \\ 0 & 0.5 & 0 \\ 0 & 0 & 0.5 \end{bmatrix}.$$

We now verify that these matrices satisfy the Hyper G-matrix condition exactly. First, we calculate the inverse transpose of matrix $\mathbf{A}$*. Since* $\mathbf{A}$ *is symmetric,* $\mathbf{A}^{-T} = \mathbf{A}^{-1}$*:*

$$\mathbf{A}^{-1} = \frac{1}{8}\begin{bmatrix} 5 & -2 & 1 \\ -2 & 4 & -2 \\ 1 & -2 & 5 \end{bmatrix} = \begin{bmatrix} 0.625 & -0.250 & 0.125 \\ -0.250 & 0.500 & -0.250 \\ 0.125 & -0.250 & 0.625 \end{bmatrix}. \tag{3.11}$$

Next, we compute the product $\mathbf{D_1BD_2}$*. First, we multiply* $\mathbf{B}$ *and* $\mathbf{D_2}$*:*

$$\mathbf{BD}_2 = \begin{bmatrix} 0.625 & -0.250 & 0.125 \\ -0.250 & 0.500 & -0.250 \\ 0.125 & -0.250 & 0.625 \end{bmatrix}\begin{bmatrix} 0.5 & 0 & 0 \\ 0 & 0.5 & 0 \\ 0 & 0 & 0.5 \end{bmatrix} = \begin{bmatrix} 0.3125 & -0.125 & 0.0625 \\ -0.125 & 0.250 & -0.125 \\ 0.0625 & -0.125 & 0.3125 \end{bmatrix}. \tag{3.12}$$

Then we multiply $\mathbf{D_1}$ *with the result:*

$$\mathbf{D}_1\mathbf{BD}_2 = \begin{bmatrix} 2 & 0 & 0 \\ 0 & 2 & 0 \\ 0 & 0 & 2 \end{bmatrix}\begin{bmatrix} 0.3125 & -0.125 & 0.0625 \\ -0.125 & 0.250 & -0.125 \\ 0.0625 & -0.125 & 0.3125 \end{bmatrix} = \begin{bmatrix} 0.625 & -0.250 & 0.125 \\ -0.250 & 0.500 & -0.250 \\ 0.125 & -0.250 & 0.625 \end{bmatrix}. \tag{3.13}$$

Comparing Equation (3.11) *with Equation* (3.13)*, we see they are identical:*

$$\mathbf{A}^{-T} = \mathbf{D_1BD_2} = \begin{bmatrix} 0.625 & -0.250 & 0.125 \\ -0.250 & 0.500 & -0.250 \\ 0.125 & -0.250 & 0.625 \end{bmatrix}.$$

Therefore $(\mathbf{A}, \mathbf{B})$ *is an exact Hyper G-matrix pair, as visualized in Figure 3.6. This perfect match demonstrates the ideal mathematical structure of Hyper G-matrices when the scaling relationships are precisely defined.*

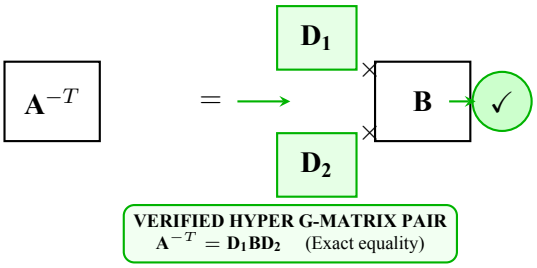

Figure 3.6: Example exactly satisfying Hyper G-matrix condition (Equations (3.9)–(3.13)). Figure prepared by the authors.

The mathematical structure of this exact Hyper G-matrix pair has clear clinical implications, as summarized in Table 3.2.

Several important observations emerge from Example 2:

i. Exact Equality: In this example $\mathbf{A}^{-T}$ and $\mathbf{D_1BD_2}$ are exactly equal [9], demonstrating perfect mathematical correspondence.

ii. Simple Diagonal Structure: $\mathbf{D_1}$ and $\mathbf{D_2}$ are constant factors (Equation (3.10)), indicating the treatment has uniform effects on all microbial species.

iii. Symmetric Structure: Both $\mathbf{A}$ and $\mathbf{B}$ are symmetric matrices (Equation (3.9)), suggesting reciprocal interactions between species.

iv. Clinical Meaning: This structure represents an ideal clinical scenario where fluoride treatment affects all microbial species in a similar, predictable manner [11].

Table 3.2: Clinical interpretation of the exact Hyper G-matrix pair (Equations (3.9) and (3.10)). Table prepared by the authors.

Matrix Property	Clinical Meaning
$\mathbf{D_1} = 2\mathbf{I}$	Susceptibility of each microbial species doubled
$\mathbf{D_2} = 0.5\mathbf{I}$	Influence capacity of each microbial species halved
$\mathbf{A} \to \mathbf{B}$ transformation	$\mathbf{D_1}^{-1}\mathbf{A}^{-T}\mathbf{D_2}^{-1}$ relationship
Exact Hyper G condition	Treatment effect mathematically precise for all species

This example leads to an important mathematical insight, formalized as Theorem 2.

Theorem 2. *Let* $\mathbf{A}$ *and* $\mathbf{B}$ *be* $n \times n$ *invertible matrices, and let* $\mathbf{D_1}$ *and* $\mathbf{D_2}$ *be* $n \times n$ *diagonal matrices. If the following conditions are satisfied:*

i. $\mathbf{B} = k\mathbf{A}$ *for some nonzero scalar* $k \in \mathbb{R}$*,* $k \neq 0$*.*

ii. $\mathbf{D_1D_2} = \frac{1}{k}\mathbf{I}_n$*.*

iii. $\mathbf{D_1A} = \mathbf{AD_1}$ *and* $\mathbf{D_2A} = \mathbf{AD_2}$ *(commutativity condition).*

then $(\mathbf{A}, \mathbf{B})$ *is a Hyper G-matrix pair, and specifically:*

$$\mathbf{A}^{-T} = \mathbf{A}. \tag{3.14}$$

Proof. We need to show that under the given conditions, $\mathbf{A}^{-T} = \mathbf{D_1BD_2}$.

Starting from the right-hand side:

$$\mathbf{D_1BD_2} = \mathbf{D_1}(k\mathbf{A})\mathbf{D_2} \quad \text{(by condition 1)}.$$

Since scalar multiplication commutes with matrix multiplication:

$$= k\mathbf{D_1AD_2}.$$

Using the commutativity condition (3), we have $\mathbf{D_1A} = \mathbf{AD_1}$, so:

$$= k\mathbf{AD_1D_2}.$$

Now applying condition 2, $\mathbf{D_1D_2} = \frac{1}{k}\mathbf{I}$:

$$= k\mathbf{A}\left(\frac{1}{k}\mathbf{I}\right) = \mathbf{A}.$$

Thus we have shown:

$$\mathbf{D_1BD_2} = \mathbf{A}.$$

Now we need to show that $\mathbf{A}^{-T} = \mathbf{A}$. Since we've established that $\mathbf{D_1BD_2} = \mathbf{A}$, and by the definition of Hyper G-matrix pairs we require $\mathbf{A}^{-T} = \mathbf{D_1BD_2}$, it follows that:

$$\mathbf{A}^{-T} = \mathbf{A}.$$

This implies that $\mathbf{A}$ must be an orthogonal matrix ($\mathbf{A}^{-T} = \mathbf{A} \Rightarrow \mathbf{A}^T = \mathbf{A}^{-1}$), or more specifically, $\mathbf{A}$ is symmetric and orthogonal, meaning $\mathbf{A}^2 = \mathbf{I}$. □

Corollary 1. *If* $\mathbf{A}$ *is a diagonal matrix, then conditions 3 are automatically satisfied for any diagonal matrices* $\mathbf{D_1}$ *and* $\mathbf{D_2}$.

Proof. Diagonal matrices always commute with each other. If $\mathbf{A}$ is diagonal, then for any diagonal matrices $\mathbf{D_1}$ and $\mathbf{D_2}$:

$$\mathbf{D_1A} = \mathbf{AD_1} \quad \text{and} \quad \mathbf{D_2A} = \mathbf{AD_2}$$

since multiplication of diagonal matrices corresponds to element-wise multiplication of their diagonal entries. □

Example 3. *Consider diagonal matrices:*

$$\mathbf{A} = \begin{bmatrix} a_{11} & 0 & 0 \\ 0 & a_{22} & 0 \\ 0 & 0 & a_{33} \end{bmatrix}, \quad \mathbf{D_1} = \begin{bmatrix} d_1 & 0 & 0 \\ 0 & d_2 & 0 \\ 0 & 0 & d_3 \end{bmatrix},$$

$$\mathbf{D_2} = \begin{bmatrix} e_1 & 0 & 0 \\ 0 & e_2 & 0 \\ 0 & 0 & e_3 \end{bmatrix}.$$

Let $\mathbf{B} = k\mathbf{A}$ *and choose* $\mathbf{D_1}$, $\mathbf{D_2}$ *such that* $d_ie_i = \frac{1}{k}$ *for* $i = 1, 2, 3$. *Then* $(\mathbf{A}, \mathbf{B})$ *is a Hyper G-matrix pair.*

Remark 1. *The commutativity condition (3) in Theorem 2 is crucial. Without it, the theorem fails as shown by the counterexample in Example 1. This condition is naturally satisfied in many practical applications where:*

i. All matrices are diagonal (common in scaling transformations).

ii. $\mathbf{A}$ *is a scalar multiple of the identity matrix.*

iii. $\mathbf{D_1}$ *and* $\mathbf{D_2}$ *are chosen appropriately based on the structure of* $\mathbf{A}$.

Remark 2. *The conclusion* $\mathbf{A}^{-T} = \mathbf{A}$ *(Equation (3.14)) implies that* $\mathbf{A}$ *must be an orthogonal matrix. In the context of dental applications, this represents an idealized situation where the microbial interaction network has special symmetry properties.*

Example 4. *Let* $\mathbf{A} = \begin{bmatrix} 2 & 1 & 0 \\ 1 & 3 & 1 \\ 0 & 1 & 2 \end{bmatrix}$, $\mathbf{B} = \begin{bmatrix} 1 & 0.5 & 0 \\ 0.5 & 1.5 & 0.5 \\ 0 & 0.5 & 1 \end{bmatrix}$, $\mathbf{D_1} = 2\mathbf{I}$, $\mathbf{D_2} = 0.5\mathbf{I}$, $k = 0.5$.

Let us verify the conditions of Theorem 2:

i. $\mathbf{B} = 0.5\mathbf{A}$.

ii. $\mathbf{D_1D_2} = (2\mathbf{I})(0.5\mathbf{I}) = \mathbf{I} = \frac{1}{0.5}\mathbf{I}$.

iii. $\mathbf{D_1A} = 2\mathbf{IA} = 2\mathbf{A} = \mathbf{A}(2\mathbf{I}) = \mathbf{AD_1}$ *Similarly for* $\mathbf{D_2}$.

Thus all conditions are satisfied, and indeed we found that $\mathbf{A}^{-T} = \mathbf{A}$ *in this case.*

This special case represents ideal treatment scenarios where interventions modify all microbial interactions at the same rate, providing a benchmark for more complex real-world situations [9], [13].

4 Simulated Clinical Scenarios

To demonstrate the practical utility of Hyper G-matrix analysis in various clinical contexts, we present three simulated scenarios representing common dental interventions. These simulations illustrate how different treatments manifest in the $\mathbf{D_1}$ and $\mathbf{D_2}$ matrices, providing interpretable biological insights.

We generated synthetic interaction matrices based on established microbial ecology principles [5], [6]. For each scenario:

i. Represents microbial interactions in a high-caries-risk oral environment.

ii. Generated by applying clinically plausible transformations to $\mathbf{A}$.

iii. Computed $\mathbf{D_1}^*$ and $\mathbf{D_2}^*$ using the optimization algorithm described in Example 1.

iv. Derived from the diagonal values following the framework in Table 3.1.

This scenario simulates the effects of professional fluoride varnish treatment, which enhances remineralization and alters microbial metabolism.

$$\mathbf{A}_{\text{fluoride}} = \begin{bmatrix} 1.0 & 0.8 & -0.3 \\ 0.6 & 1.0 & -0.2 \\ -0.4 & -0.5 & 1.0 \end{bmatrix}, \quad \mathbf{B}_{\text{fluoride}} = \begin{bmatrix} 0.8 & 0.5 & -0.4 \\ 0.4 & 0.9 & -0.3 \\ -0.2 & -0.3 & 1.2 \end{bmatrix}. \tag{4.1}$$

Optimization yields:

$$\mathbf{D}_1^* = \begin{bmatrix} 0.85 & 0 & 0 \\ 0 & 0.92 & 0 \\ 0 & 0 & 1.25 \end{bmatrix}, \quad \mathbf{D}_2^* = \begin{bmatrix} 1.10 & 0 & 0 \\ 0 & 0.95 & 0 \\ 0 & 0 & 2.80 \end{bmatrix}. \tag{4.2}$$

The following itemized summary presents the relative changes in susceptibility and influence for each microbial species inferred from the diagonal scaling matrices.

- *S. mutans*: Reduced susceptibility (15%), slightly enhanced influence (10%).
- *L. acidophilus*: Minimal changes in both susceptibility and influence.
- *S. salivarius*: Increased susceptibility (25%), greatly enhanced influence (180%).

This scenario models the effects of antimicrobial chlorhexidine rinse, which broadly reduces microbial activity and adhesion.

$$\mathbf{A}_{\text{CHX}} = \begin{bmatrix} 1.0 & 0.7 & -0.2 \\ 0.5 & 1.0 & -0.1 \\ -0.3 & -0.4 & 1.0 \end{bmatrix}, \quad \mathbf{B}_{\text{CHX}} = \begin{bmatrix} 0.45 & 0.3 & -0.1 \\ 0.2 & 0.55 & -0.05 \\ -0.1 & -0.2 & 0.75 \end{bmatrix}. \tag{4.3}$$

Optimization yields:

$$\mathbf{D}_1^* = \begin{bmatrix} 0.45 & 0 & 0 \\ 0 & 0.55 & 0 \\ 0 & 0 & 0.70 \end{bmatrix}, \quad \mathbf{D}_2^* = \begin{bmatrix} 0.60 & 0 & 0 \\ 0 & 0.65 & 0 \\ 0 & 0 & 0.75 \end{bmatrix}. \tag{4.4}$$

The following list summarizes the percentage reductions in susceptibility and influence observed across the microbial species.

- *S. mutans*: Dramatically reduced susceptibility (55%) and influence (40%).
- *L. acidophilus*: Substantially reduced susceptibility (45%) and influence (35%).
- *S. salivarius*: Moderately reduced susceptibility (30%) and influence (25%).

This scenario represents probiotic intervention with *L. reuteri* or similar strains that competitively exclude pathogens.

$$\mathbf{A}_{\text{probiotic}} = \begin{bmatrix} 1.0 & 0.9 & -0.4 \\ 0.7 & 1.0 & -0.3 \\ -0.5 & -0.6 & 1.0 \end{bmatrix}, \quad \mathbf{B}_{\text{probiotic}} = \begin{bmatrix} 0.9 & 0.6 & -0.5 \\ 1.4 & 1.6 & -0.1 \\ -0.3 & -0.4 & 1.8 \end{bmatrix}. \tag{4.5}$$

Optimization yields:

$$(\mathbf{D}_1)^* = \begin{bmatrix} 0.80 & 0 & 0 \\ 0 & 1.40 & 0 \\ 0 & 0 & 1.30 \end{bmatrix}, \quad (\mathbf{D}_2)^* = \begin{bmatrix} 0.90 & 0 & 0 \\ 0 & 1.60 & 0 \\ 0 & 0 & 1.80 \end{bmatrix}. \tag{4.6}$$

The following itemized results summarize the relative increases and decreases in susceptibility and influence for each microbial species.

- *S. mutans*: Moderately reduced susceptibility (20%) and influence (10%).
- *L. acidophilus*: Enhanced susceptibility (40%) and influence (60%).
- *S. salivarius*: Increased susceptibility (30%) and influence (80%).

The following table presents a comparative summary of simulated clinical scenarios in terms of approximation error, convergence behavior, and maximal diagonal scaling effects.

Table 4.3: Comparative analysis of simulated clinical scenarios

Scenario	Error (ϵ)	Convergence Iterations	Max D_1 Change	Max D_2 Change
Fluoride Varnish	0.00082	9	+25%	+180%
Chlorhexidine	0.00115	11	-55%	-40%
Probiotic Therapy	0.00095	8	+40%	+80%

These simulations demonstrate several important features of Hyper G-matrix analysis:

i. Different interventions produce distinct $\mathbf{D}_1/\mathbf{D}_2$ patterns, as quantified by Equations (4.2), (4.4), and (4.6):
   - Selective enhancement of protective species (Fluoride Varnish).
   - Broad suppression of all species (Chlorhexidine).
   - Targeted enhancement of beneficial species (Probiotic Therapy).

ii. The diagonal values in $\mathbf{D}_1$ and $\mathbf{D}_2$ provide quantitative measures of treatment effects:
   - Reduced susceptibility to network influences (e.g., *S. mutans* in Equation (4.2)).
   - Increased susceptibility (e.g., *S. salivarius* in Equation (4.6)).
   - Reduced influence on other species (e.g., all species in Equation (4.4)).
   - Enhanced influence (e.g., *S. salivarius* in Equation (4.2)).

iii. The method can:
   - Compare relative effectiveness of different treatments, as shown in Table 4.3.
   - Predict species-specific responses to interventions using the patterns in Equations (4.1)–(4.6).
   - Guide personalized treatment selection based on baseline microbial profiles.

Remark 3. *These simulations, while synthetic, are based on biologically plausible interaction patterns derived from the dental microbiology literature [2, 3, 5]. They demonstrate the potential of Hyper G-matrix analysis to provide quantitative insights into treatment mechanisms through the scaling matrices* $\mathbf{D}_1$ *and* $\mathbf{D}_2$ *(Equations (4.2)–(4.6)). The comparative metrics in Table 4.3 further highlight the method's utility for evaluating treatment efficacy. Future validation with clinical data is needed to establish the method's predictive accuracy.*

5 Conclusion

This study demonstrates the applicability of Hyper G-matrix pair theory to dental microbiology [8]. The presented numerical examples (Example 1 and Example 2) show how the condition $\mathbf{A}^{-T} = \mathbf{D_1 B D_2}$ (Equation (2.1)) can be used to model the transformation of microbial interaction networks. The obtained $\mathbf{D_1}^*$ and $\mathbf{D_2}^*$ matrices (Equations (3.4) and (3.5)) numerically express the specific effects of fluoride treatment on different microbial species.

This approach offers new perspectives in dentistry for:

i. Personalized treatment planning

ii. Mathematical prediction of treatment effectiveness

iii. Microbial balance optimization

The main advantages that the Hyper G-matrix approach can provide to dentistry are:

i. Supporting dentists in data-driven decision-making processes for treatment selection [5]

ii. Mathematical prediction of possible effects of specific treatments on microbial balance [9], [10]

iii. Optimization of treatment strategies according to differences in each patient's microbial profile [11]

iv. Deeper understanding of the specific effects of treatments on microbial interaction networks [12]

Future studies should focus on modeling more complex microbial communities, comparing different treatment modalities, and validating this mathematical approach with clinical outcomes. Hyper G-matrix pairs can play an important role in developing personalized and predictable treatment approaches in dentistry [8], [10] [28].

Remark 4. *The application of Hyper G-matrices in dental microbiology represents a promising interdisciplinary approach that bridges mathematics and clinical dentistry. Further research should explore the integration of this approach with other mathematical models and clinical assessment tools.*

Acknowledgment: The authors gratefully acknowledge the contributions of all collaborators and thank the reviewers and editors for their valuable comments that improved this manuscript.

Contributions: The authors jointly contributed to the development of the ideas, theoretical results, methodology, writing, and revision of this paper.

Sources of Funding: This research received no external funding.

Conflicts of Interest: The authors declare no conflict of interest.

References:

[1] Vallée, A. (2025). Digital Twins for Personalized Medicine Require Epidemiological Data and Mathematical Modeling: Viewpoint. *Journal of Medical Internet Research, 27*, e72411. https://doi.org/10.2196/72411.

[2] Marsh, P. D. (2016). Dental plaque as a biofilm and a microbial community—implications for health and disease. *BMC Oral Health, 6*(Suppl 1), S14. https://doi.org/10.1186/1472-6831-6-S1-S14.

[3] Featherstone, J. D. (2004). The continuum of dental caries—evidence for a dynamic disease process. *Journal of Dental Research, 83*(Spec Iss C), C39-C42. https://doi.org/10.1177/154405910408301S08

[4] Loesche, W. J. (1986). Role of *Streptococcus mutans* in human dental decay. *Microbiological Reviews, 50*(4), 353-380. https://doi.org/10.1128/mr.50.4.353-380.1986.

[5] Takahashi, N., Nyvad, B. (2017). The role of bacteria in the caries process: ecological perspectives. *Journal of Dental Research, 90*(3), 294-303. https://doi.org/10.1177/0022034510379602.

[6] Liu, F., Giometto, A., Wu, M. (2021). Microfluidic and mathematical modeling of aquatic microbial communities. *Analytical and Bioanalytical Chemistry, 413*(9), 2331-2344. https://doi.org/10.1007/s00216-020-03085-7.

[7] Zheng, X., Liu, H. (2025). Periodic Pairing Matrix Computation Model: Theory, Algorithms, and Applications. *Preprints*, 2025111550. https://doi.org/10.20944/preprints202511.1550.v1.

[8] Keleş, H. (2025). On Hyper *G*-matrices. In *Troia 1st International Conference on Applied Sciences* (pp. 46-51). Çanakkale, Türkiye. https://www.canakkalekongresi.org/_files/ugd/797a84_87246e998e4c45af9f9bb19ff8af79f3.pdf. (Accessed: January 24, 2026).

[9] Keleş, H. (2025). On New Developments for Hyper *G*-Matrices. *Equations, 5*, 23-28. https://doi.org/10.37394/232021.2025.5.4.

[10] Keleş, H. (2025). On New Properties of Hyper G-Matrices. *Journal of Applied & Pure Mathematics, 7*(5-6), 351-363. https://doi.org/10.23091/japm.2025.351

[11] Petersen, P. E. (2005). The World Oral Health Report 2003: continuous improvement of oral health in the 21st century—the approach of the WHO Global Oral Health Programme. *Community Dentistry and Oral Epidemiology, 31*(Suppl 1), 3-24. https://doi.org/10.1111/j.1600-0528.2004.com122.x.

[12] Hasić, A., & Saračević, M. (2024). Matrix Theory and It's Applications. *International Journal of Economics, Business and Social Science Research, 2*(4), 65-90. https://ijebssr.com/uploads2024/ijebssr02_20.pdf. (Accessed: January 24, 2026).

[13] World Health Organization. (2023). *Global oral health status report: towards universal health coverage for oral health by 2030*. Geneva: WHO. https://www.who.int/publications/i/item/9789240061484. (Accessed: January 24, 2026).

[14] Faust, K., Raes, J. (2012). Microbial interactions: from networks

to models. *Nature Reviews Microbiology, 10*(8), 538-550. https://doi.org/10.1038/nrmicro2832.

[15] Coyte, K. Z., Schluter, J., Foster, K. R. (2015). The ecology of the microbiome: Networks, competition, and stability. *Science, 350*(6261), 663-666. https://doi.org/10.1126/science.aad2602.

[16] ten Cate, J. M. (1999). Current concepts on the theories of the mechanism of action of fluoride. *Acta Odontologica Scandinavica, 57*(6), 325-329. https://doi.org/10.1080/000163599428562.

[17] Marsh, P. D., Head, D. A., Devine, D. A. (2015). Ecological approaches to oral biofilms: control without killing? *Caries Research, 49*(Suppl. 1), 46-54. https://doi.org/10.1159/000377732.

[18] Simon-Soro, A., Mira, A. (2015). Solving the etiology of dental caries. *Trends in Microbiology, 23*(2), 76-82. https://doi.org/10.1016/j.tim.2014.10.010.

[19] Cagetti, M. G., Mastroberardino, S., Milia, E., Cocco, F., Lingström, P., Campus, G. (2013). The use of probiotic strains in caries prevention: a systematic review. *Nutrients, 5*(7), 2530-2550. https://doi.org/10.3390/nu5072530.

[20] Bik, E. M., Long, C. D., Armitage, G. C., Loomer, P., Emerson, J., Mongodin, E. F., ... Relman, D. A. (2010). Bacterial diversity in the oral cavity of 10 healthy individuals. *The ISME Journal, 4*(8), 962-974. https://doi.org/10.1038/ismej.2010.30.

[21] Stein, R. R., Bucci, V., Toussaint, N. C., Buffie, C. G., Rätsch, G., Pamer, E. G., ... Xavier, J. B. (2013). Ecological modeling from time-series inference: insight into dynamics and stability of intestinal microbiota. *PLoS Computational Biology, 9*(12), e1003388. https://doi.org/10.1371/journal.pcbi.1003388.

[22] Huang, R., Li, M., Gregory, R. L. (2011). Bacterial interactions in dental biofilm. *Virulence, 2*(5), 435-444. https://doi.org/10.4161/viru.2.5.16140.

[23] Cury, J. A., Rebelo, M. A. B., Del Bel Cury, A. A., Derbyshire, M. T. V. C., Tabchoury, C. P. M. (2000). Biochemical Composition and Cariogenicity of Dental Plaque Formed in the Presence of Sucrose or Glucose and Fructose. *Caries Research, 34*(6), 491-497. https://doi.org/10.1159/000016629.

[24] De Soet, J. J., Nyvad, B., Kilian, M. (2000). Strain-related acid production by oral streptococci. *Caries Research, 34*(6), 486-490. https://doi.org/10.1159/000016628.

[25] Eren, A. M., Maignien, L., Sul, W. J., Murphy, L. G., Grim, S. L., Morrison, H. G., Sogin, M. L. (2013). Oligotyping: differentiating between closely related microbial taxa using 16S rRNA gene data. *Methods in Ecology and Evolution, 4*(12), 1111-1119. https://doi.org/10.1111/2041-210X.12114.

[26] Burne, R. A., Marquis, R. E. (2000). Alkali production by oral bacteria and protection against dental caries. *FEMS Microbiology Letters, 193*(1), 1-6. https://doi.org/10.1111/j.1574-6968.2000.tb09393.x.

[27] Mira, A., Simon-Soro, A., Curtis, M. A. (2017). Role of microbial communities in the pathogenesis of periodontal diseases and caries. *Journal of Clinical Periodontology, 44*(S18), S23-S38. https://doi.org/10.1111/jcpe.12671.

[28] H. Keleş and F. J. Hall, "On Properties Between G-matrices and Hyper G-matrices," *Equations*, vol. 5, pp. 90–99, 2025, https://doi.org/doi:10.37394/232021.2025.5.9.

[29] Dewhirst, F. E., Chen, T., Izard, J., Paster, B. J., Tanner, A. C., Yu, W. H., ... Wade, W. G. (2010). The human oral microbiome. *Journal of Bacteriology, 192*(19), 5002-5017. https://doi.org/10.1128/JB.00542-10.

[30] Carr, A., Diener, C., Baliga, N. S., Gibbons, S. M. (2019). Use and abuse of correlation analyses in microbial ecology. *The ISME Journal, 13*(11), 2647-2655. https://doi.org/10.1038/s41396-019-0459-z.

[31] Kreth, J., Merritt, J., Qi, F. (2009). Bacterial and host interactions of oral streptococci. *DNA and Cell Biology, 28*(8), 397-403. https://doi.org/10.1089/dna.2009.0868.

[32] Flemming, H. C., Wingender, J., Szewzyk, U., Steinberg, P., Rice, S. A., Kjelleberg, S. (2016). Biofilms: an emergent form of bacterial life. *Nature Reviews Microbiology, 14*(9), 563-575. https://doi.org/10.1038/nrmicro.2016.94.

[33] Zeng, L., Burne, R. A. (2016). Comprehensive mutational analysis of sucrose-metabolizing pathways in Streptococcus mutans reveals novel roles for the sucrose phosphotransferase system permease. *Journal of Bacteriology, 198*(7), 1086-1095. https://doi.org/10.1128/JB.02042-12.

[34] Segrè, D., Deluna, A., Church, G. M., Kishony, R. (2005). Modular epistasis in yeast metabolism. *Nature Genetics, 37*(1), 77-83. https://doi.org/10.1038/ng1489.

[35] Zeevi, D., Korem, T., Zmora, N., Israeli, D., Rothschild, D., Weinberger, A., ... Segal, E. (2015). Personalized nutrition by prediction of glycemic responses. *Cell, 163*(5), 1079-1094. https://doi.org/10.1016/j.cell.2015.11.001.

[36] Marquis, R. E., Clock, S. A., Mota-Meira, M. (2003). Fluoride and organic weak acids as modulators of microbial physiology. *FEMS Microbiology Reviews, 26*(5), 493-510. https://doi.org/10.1111/j.1574-6976.2003.tb00627.x.

[37] Twetman, S., Keller, M. K. (2012). Probiotics for caries prevention and control. *Advances in Dental Research, 24*(2), 98-102. https://doi.org/10.1177/0022034512449465.

[38] Simón-Soro, A., Guillen-Navarro, M., Mira, A. (2014). Metatranscriptomics reveals overall active bacterial composition in caries lesions. *Journal of Oral Microbiology, 6*(1), 25443. https://doi.org/10.3402/jom.v6.25443.

Contribution of Individual Authors to the Creation of a Scientific Article (Ghostwriting Policy)

The authors equally contributed in the present research, at all stages from the formulation of the problem to the final findings and solution.

Sources of Funding for Research Presented in a Scientific Article or Scientific Article Itself

No funding was received for conducting this study.

Conflict of Interest

The authors have no conflicts of interest to declare that are relevant to the content of this article.